한국뇌학회지, Vol. 2, No. 1, pp. 19−35, June 2002

바이퍼캐이팅 뉴런 네트워크

이기혁
한국정보통신대학교

Bifurcating Neuron Networks

Geehyuk Lee
School of Engineering, Information & communications University, Daejeon, 305-380, Korea

Abstract: Among many newly raised issues in neuroscience, we have been particularly interested in three issues, time coding, the role of coherent activities, and the role of chaotic activities. The Bifurcating Neuron (BN) is our model neuron designed with these three issues in mind: it is a chaotic neuron that can deal with time coding and has a built-in mechanism to incorporate the influence of coherent activity in its environment. The Bifurcating Neuron Network 1 (BNN-1) is a binary associative memory based on chaotic attractors. The BNN-1, utilizing the bistability of the BN controlled by attractor-merging crisis, was shown to have a better recall ability than the continuous-time Hopfield network. The BNN-1 is particularly suited for circuit realization because the only required circuit components are relaxation oscillators and harmonic oscillators. Another feature of the BNN-1 is that its chaotic activity is self-organizing: it starts in a maximally chaotic state and settles down to a less chaotic state as a recall process proceeds. The BN Network 2 (BNN-2) is another BN network that is designed to store analog patterns. It is based on the amplitude-to-phase transformation characteristics of the BN and the constructive interference, in the sense of wave optics, among neuronal spikes. A Hebbian learning scheme results in the formation of attractors with large basins of attraction. Also, the firing-time pattern of BNs induced by the same input pattern becomes different when the frequency of the relaxation level oscillation changes, and this led us to consider the possibility of volume-holographic memory. In a numerical simulation, we could configure the BNN-2 to maintain memories of two sets of patterns, one of which becomes accessible when the frequency of the relaxation level oscillation is tuned to that of the recording phase.

Key words: integrate-and-fire neurons, pulse-coupled neural networks, bifurcating neurons, bifurcating neuron networks, temporal coding, coherent activities, chaos, associative memory.

요 약: 최근 뇌과학 분야에서 관심을 모으는 여러 가지 이슈 중, 우리는 time coding, coherent activity의 역할, chaotic activity의 역할 등의 세 가지에 특별한 관심을 가지고 있다. Bifurcating Neuron (BN)은 이러한 세 가지 이슈를 염두에 두고 개발된 독자적인 뉴런 모델이다. 즉, BN은 time coding을 기반으로 하여, 신경망 내에서의 coherent activity의 영향을 반영하는 모델이다. Bifurcating Neuron Network 1 (BNN-1) 은 chaotic attractor를 기반으로 한 이진 연상메모리이다. BNN-1은 attractor-merging crisis의 지배 하에 있는 BN의 bistability를 이용함으로 해서 continuous-time Hopfield network보다 우수한 연상능력을 보여주고 있다. 또한, BNN-1은 relaxation oscillator와 harmonic oscillator만으로 구현이 가능한 장점을 가지고 있다. 또 다른 장점은 BNN-1의 chaotic activity가 self-organizing하다는 점을 들 수 있다. 즉, 연상 초기에는 지극히 chaotic한 상태에서 시작하여 연상작용이 완료됨에 따라 보다 덜 chaotic한 상태로 전이한다. 이러한 BNN-1의 특성은 특히 BNN-1을 optimization problem의 해법에 응용할 때 특히 유용하다. Bifurcating Neuron Network 2 (BNN-2)는 또 다른 BN을 기반으로 하는 연상메모리로서, 아날로그 패턴을 저장할 수 있다. BNN-2는 BN의 amplitude-to-phase 변환특성과 뉴런 펄스의 보강간섭원리를 이용하고 있다. Hebbian learning에 따라 여러 가지 패턴을 저장할 수 있으며, 각각의 패턴은 네트워크 상태공간에서 큰 basin을 가진 attractor를 형성한다. 또한, BN

교신저자: 이기혁
한국정보통신대학교, 305-380 대전광역시 유성구 문지동 103-6
Tel: 042-866-6705
Fax: 042-866-6745
E-mail: geehyuk@icu.ac.kr

으로부터의 출력 펄스 열이 coherent activity의 주파수에 따라 달라지므로, BNN-2는 volume holography와 유사한 특성을 가지게 된다. 수치해석을 이용한 시뮬레이션에서 BNN-2가 두 가지 그룹의 패턴들을 coherent activity의 주파수를 달리하여 독립적으로 기억, 연상할 수 있음을 확인할 수 있었다.

주요어: integrate-and-fire 뉴런, pulse-coupled 신경망, bifurcating 뉴런, bifurcating 신경망, temporal coding, coherent activities, 혼돈, 연상메모리.

INTRODUCTION

There has been a continuing debate on the way information is encoded in neuronal spike trains. Rate coding, the most widely accepted coding scheme assumes that information is represented by the mean firing rate of a neuron (1). Rate coding has proven to be valid in some neuronal information paths, e.g., in sensory neurons and motor neurons, but its validity in other parts of the brain is questionable. Recent experimental studies are revealing a growing number of new facts beyond the explanation of rate coding and are suggesting the possibility of information coding in the precise timing of neuronal spikes, namely, time coding (2). An especially descriptive example supporting time coding in the brain is provided by O' Keefe and Recce (3), who studied the firing behavior of hippocampal place cells (4). They showed that the firing phases of place cells with respect to a theta rhythm have a high level of correlation with the animal' s location on a linear runway.

Another topic of growing interest is the role of coherent activities in the brain, especially those in the gamma-band centered around 40Hz. Some of the early observations of gamma-band oscillatory activities were made in the olfactory bulb and cortex of the rabbit (5), in the olfactory systems of the cat and the rat (6), in a variety of structures of the cat brain (6), in the cat primary visual cortex (7) (8), in the monkey visual cortex (9), and in EEG recordings from the human skull above association and motor areas (10). The observation of a synchronous activity in the cat visual cortex by Gray and Singer (7) has been drawing special attention because, in their experiments, the synchronous activity was stimulus-specific and was observed across cortical regions, e.g., across multiple visual association areas, with a small phase variation. Gray and Singer related their result to the so called feature-binding hypothesis (11) (12), which states that synchrony provides a means to bind together in time the features that represent a particular stimulus. The searchlight hypothesis of Crick (13) is another speculation on the role of synchronous activity in relation to the question of consciousness.

Yet another topic of growing interest in neuroscience is the role of chaotic activities in the brain. Different levels of chaotic activities have been observed in many experimental studies of electroencephalogram (EEG) signals, for example, in the simian motor cortex (14), in the human brain during a sleep cycle (15) and during an epileptic seizure (16), and in the olfactory bulb of the rabbit (5) (17). The mounting evidence of chaotic activities in the brain triggered much theoretical reflection on the possible role of chaotic activities in brain functions (18) (19) (20) (21). For instance, Freeman and his coworkers (5) observed in a study of the olfactory system of the rabbit that the nervous activity of the olfactory system switches from a chaotic to a periodic state whenever a familiar odor is detected. This experimental observation stimulated their reflection on the role of chaos in perception processes and led them to postulate that chaos can serve as the ground state of a perception process, i.e., an elevated state that has quick transition routes to many periodic states.

A question that has concerned us ever since we were introduced to the aforementioned topics is this: what would become possible where these three topics

converge? In other words, what would be the potential of an artificial neural network that is based on time coding and, at the same time, utilizes both coherence and chaos? In order to investigate this question, we started with the integrate-and-fire neuron (22), the simplest, time-coding-aware model neuron, and introduced coherence and chaos into the model.

In order to introduce coherence into our model neuron, we needed to define first the role of coherence. The one that we chose over others is that coherent activities in a network can provide a common time reference to the constituent neurons. This role of coherence may sound excessively general or even trivial but is certainly essential because, in the absence of a time reference, the information that time coding can carry would be quite limited. The aforementioned O'Keefe and Recce experiment (3) is a good example for such a role of coherence (the theta rhythm). The fact that rate coding is common in sensory or motor neurons is also consistent with such a role of coherence: rate coding must be the only choice when a common time reference extending throughout the nervous system is not available. As a way to provide a time reference, we introduced a common sinusoidal oscillation to the relaxation level of the integrate-and-fire neuron.

The second goal of introducing chaos into our model neuron was achieved at the same time as we introduced a sinusoidal oscillation to the relaxation level of the integrate-and-fire neuron. The resultant neuron, which we call a bifurcating neuron (BN), has the intrinsic ability to switch between a regular and a chaotic state as the amplitude of the relaxation level oscillation changes. We expected the chaotic activities observed in the BN would be useful in the "ready-state" of a network where the network is ready to respond to an external stimulus. We have the following scenario in mind for our design of BN networks: a stimulus known to a network causes the interconnections in the network to interfere constructively, and thereby suppress the initial chaotic activity in the network. This scenario is in fact inspired by the experimental observation of Freeman and Skarda (5) and also by some recent studies that show that the behavior of individual neurons in isolation is more irregular than that of neurons in a network (23).

In the following sections, we introduce the BN and two distinct types of BN networks, the Bifurcating Neuron Network 1 (BNN-1) and the Bifurcating Neuron Network 2 (BNN-2). These networks will demonstrate what kind of computation can become possible when time-coding-aware model neurons cooperate under a common time reference.

THE BIFURCATING NEURON

A neuron in a neural network receives inputs from many different parts of the brain and is also subject to noise from inside and outside. Also, the same input can have different effects depending on the nature and the position of the synapse. Consideration of every detail of the interaction of a neuron with its environment would be impractical, so, we made the following rather simplistic assumptions about the artificial environment surrounding an integrate-and-fire neuron. First, the environment provides a persistent incoherent input to the neuron, which helps the neuron keep active at an optimal operating point. Second, the environment also provides a persistent coherent input to the neuron, which is common to all the neurons in the same network and serves as a time reference. The BN, an integrate-and-fire neuron augmented by such inputs from the environment, is defined by the following set of equations:

$$\frac{dx}{dt} = c,\ \theta(t) = 1,\ \rho(t) = -\rho_o \sin 2\pi f t \qquad (1)$$

where x, θ and ρ are the internal potential, the threshold level, and the relaxation level of a BN, respectively, c is the buildup rate of the internal potential, and ρ_o and f are the amplitude and frequency of the relaxation level oscillation. Figure 1

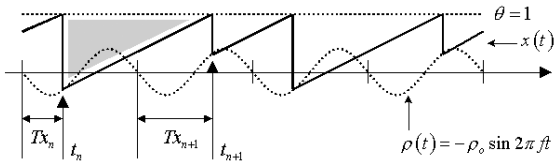

Figure 1 The time evolution of the BN: the recurrent relation between the successive firing times $t(n)$ and $t(n+1)$ can be derived by considering the ratio of the two perpendicular sides of the shaded triangle.

depicts the behavior of the BN: it keeps firing due to an incoherent source while the relaxation level is oscillating due to a coherent source. The recurrent relation between the successive firing times $t(n+1)$ and $t(n)$ can be derived by considering the ratio of the two perpendicular sides of the shaded triangle:

$$t_{n+1} = t_n + \frac{1}{c} + \frac{\rho_o}{c}\sin 2\pi f t(n) \qquad (2)$$

An important point to emphasize again here is that the coherent source serves as a time reference to the neuron. This point is clearly demonstrated in the bifurcation diagram in Fig. 2, that shows the firing times of the neuron with respect to a modulus of 1, which is the period of the sinusoidal oscillation of the relaxation level. Although the firing of the BN here is not always phase-locked to the sinusoidal oscillation, the firing time exhibits a clear structure when it is represented relative to the sinusoidal oscillation. As well as providing a time reference, the coherent source turns the neuron into a chaotic neuron. This fact is also demonstrated in Fig. 2, where one can see that the firing pattern is bifurcating until it becomes chaotic as the amplitude of the sinusoidal oscillation increases.

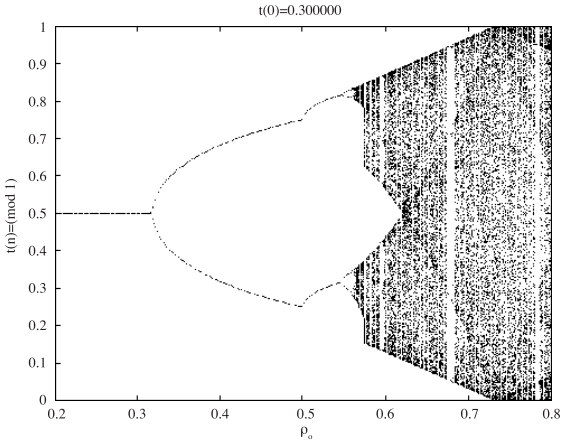

Figure 2 The bifurcation diagram of the BN for $c = f = 1$: the bifurcation parameter here is the amplitude ρ_o of the sinusoidal oscillation in the relaxation level. The vertical axis shows the firing times of the BN in the sense of modulus 1.

THE BIFURCATING NEURON NETWORK 1

The BNN-1 is a binary associative memory exploiting the bistability of the BN which appears when the average firing frequency of a BN is half that of the relaxation level oscillation. The two chaotic attractors which account for the bistability are subject to attractor-merging crisis (24). Merging or separation of the two attractors is critically dependent on the amplitude of the relaxation level oscillation. Near the point of crisis, a sinusoidal perturbation in the threshold level induced by an incoming spike train can bias the bistability, thereby inducing a binary transition. The result is a binary associative memory where a memory is represented by a chaotic attractor.

Bistability and Attractor-Merging Crisis of the BN

Under a certain combination of parameters, the BN exhibits bistability and attractor-merging crisis due to the translational symmetry of the BN. If we change

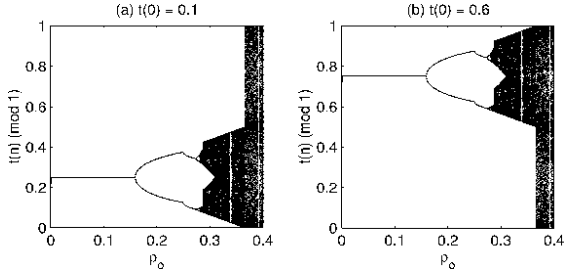

Figure 3 The bifurcation diagrams of the BN for $f = 2$: the bifurcation parameter here is the amplitude ρ_o of the sinusoidal oscillation in the relaxation level. The vertical axis shows the firing times of the BN in the sense of modulus 1.

every occurrence of t_n to t_n+1/f in the recurrent relation (2), the equation remains unchanged. Figure 3 shows the bifurcation diagrams of the BN when $f=2$. There are two symmetric attractors which divide the entire state space [0,1), in the sense of a modulus of 1, into two equal intervals. There is an unstable fixed point at $t=0.5$, whch is separating the two attractors. When the attractors expand until it touches the unstable fixed point, they undergoes a crisis and collapse into a single fully chaotic attractor. The value of the bifurcation parameter ρ_o at which the attractor-merging crisis takes place is called a crisis point $\rho_o^c \doteq 0.3663$. The bistability due to the two symmetric attractors is, in fact, a special case of the multi-stability of the BN. When $f=3$, the BN has three symmetric attractors, thereby exhibiting tri-stability. Obviously, as f is increased further, the BN will come to exhibit multi-stability.

Controlling the Bistability of the BN

Now that we have found that the BN has bistability and exhibits attractor-merging crisis, the next question is how to couple them together to form a network. What we need now is a coupling scheme that can break the translational symmetry of the BN in order to control the bistability. Suppose we introduce a sinusoidal oscillation at the threshold level, which is half the frequency of that of the relaxation level oscillation. Figure 4 shows the behavior of the BN for three different amplitudes of the threshold oscillation. In all the three cases, it is assumed that the driving amplitude ρ_o is a little higher than the crisis point. This means that, in case (b), the BN will be in a fully chaotic state and can fire at any point in the state space [0,1) in the sense of a modulus of 1. In case (a), the symmetry that gives rise to the two symmetric chaotic attractors of the BN is now broken. As a result, the first half of the state space becomes more stable than the second half, thereby the BN is more likely to fire in the first half than in the second half. The situation is reversed in case (c). The bottom line is that the translation symmetry of the BN is broken by the sinusoidal oscillation of the threshold level. In other words, the preference of the BN over the two symmetric attractors can be controlled by the threshold level oscillation. The bifurcation diagrams in Fig. 5 summarizes the behavior of the BN in response to the change in $\varepsilon = \theta(0)$. It is interesting to note that the overall shape of the bifurcation diagram tends to recall the sigmoidal curve.

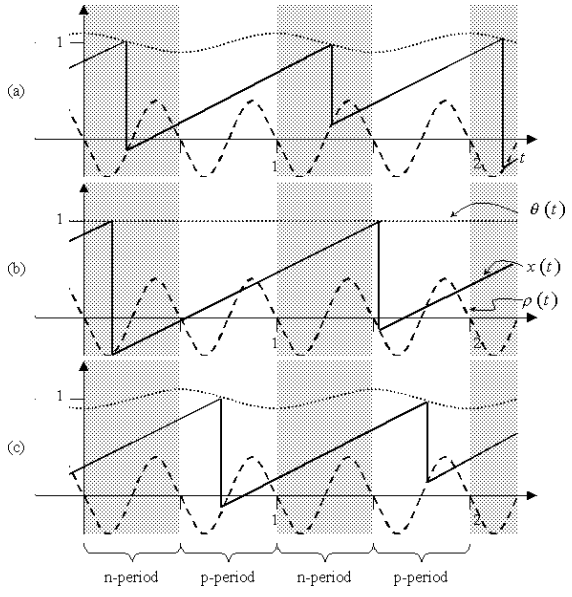

Figure 4 Breaking the translational symmetry of the BN: (a) n-periods become more stable when $\varepsilon = \theta(0) > 0$, (b) n-periods and p-periods are equally unstable when $\varepsilon = 0$, and (c) p-periods become more stable when $\varepsilon < 0$.

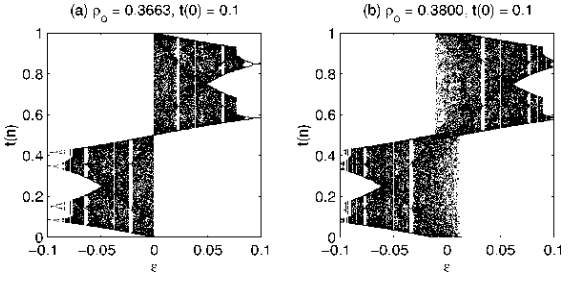

Figure 5 The bifurcation diagrams of the BN as the amplitude of threshold level changes: (a) when ρ_o is exactly at ρ_c, and (b) when ρ_o is slightly greater than ρ_c. These two bifurcation diagrams are reminiscent of the sigmoidal curve.

For the further discussion of the bistability of the BN, we need to define the binary state of the BN. The BN is considered to be in the negative state if it is firing in the first half of the state space with respect to a modulus 1. Likewise, it is considered to be in the positive state if it is firing in the second half. The precise definition of the binary state of the BN is given by

$$s(t) \equiv \begin{cases} -1 & t(n) \in [0, 0.5) (\mathrm{mod}\, 1) \\ 1 & t(n) \in [0.5, 1) (\mathrm{mod}\, 1) \end{cases} \quad (3)$$

where $t(n)$ is the last firing time of the BN before t. For ease of illustration, we call the first half and the second half of the state space as n-period and p-period, respectively. Since the two periods are defined with respect to a modulus 1, they will divide the time axis into an alternating series of n-periods and p-periods, as illustrated in Figure 4.

Pulse-Coupling via a Harmonic Oscillator

We have seen that the symmetry of the BN can be broken by in introduction of threshold level oscillation and its bistability can be controlled by the oscillation amplitude. However, the input that a BN receives from the presynaptic BNs is in the form of a spike train. Apparently, we need to provide a linkage between the spike train and the threshold level oscillation. For this purpose, we propose that the threshold level of the BN be modeled by the harmonic oscillator that is subject to an impulsive input:

$$\frac{d^2\theta_i}{dt^2} + \gamma \frac{d\theta_i}{dt} + \omega_o^2(\theta_i - 1) = u(t) \quad (4)$$

where $\omega_o = 2\pi / \sqrt{1 - 1/4Q^2}$, $\gamma = \omega_o / Q$, and Q is the Q-factor of the harmonic oscillator. The spiky input $u(t)$ from the presynaptic BNs is driving the harmonic oscillator. Note that the oscillator parameters are carefully chosen so that the oscillation frequency is 1 when the oscillator is under-damped.

Figure 6 shows a small example network to illustrate the operation of the proposed pulse-coupling scheme. The solid lines between BNs represent excitatory connections, while the dashed lines represent inhibitory connections. Suppose that the BNs are divided into two groups: three BNs firing in the n-period and the other three BNs firing in the p-period. The first temporal plot shows the expected state evolution of one of the BNs in the first group. The thick downward arrows represent the spike input from the BNs in the same group, while the thick upward arrows represent the spike input from the BNs in the other group. These inputs together will induce sinusoidal oscillation of the threshold level, as shown in the plot, and the oscillation is in such a phase as to reinforce the firing of the BN in the n-periods. The second temporal plot shows the expected state evolution of a BN in the second group. The situation is similar to that of the first plot, but this time, the resulting sinusoidal threshold level is in such phase as to reinforce the firing of the BN in the p-periods. In conclusion, the pulse-coupling scheme seems to maintain the clustering of a network into such two groups. Of course, as one can see in the figure, the

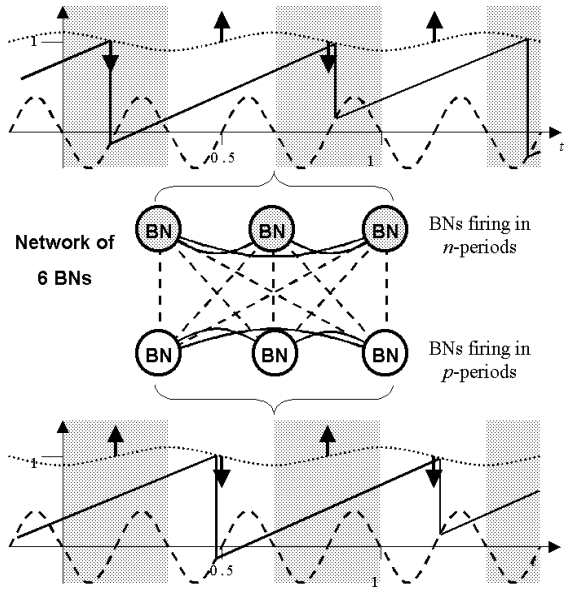

Figure 6 A small example network to illustrate the proposed pulse-coupling scheme: the upper three BNs are in the n-period and the other three are in the p-period. The solid lines between them represent excitatory connections, while the dashed lines represent inhibitory connections.

two groups are determined by the configuration of the excitatory and inhibitory connections.

Binary Associative Memory

A BNN-1 consists of I BNs that is governed by the following equation:

$$\frac{dx_i}{dt} = 1, \; i = 1,2,...,I \tag{5}$$

The state variable $x_i(t)$ increases linearly until it reaches the threshold level $\theta_i(t)$ and then drops down to the relaxation level $\rho_i(t)$. All the BNs in the network have the same relaxation level:

$$\rho_i(t) = -\rho_o \sin 4\pi t \tag{6}$$

A spike train out of a BN can be represented by a series of Dirac-delta functions:

$$y_i(t) = \sum_{n=1}^{\infty} \delta(t - t_i(n)) \tag{7}$$

where $t_i(t)$ is the n-th firing time of BN i. The weighed sum of the spike trains from the pre-synaptic BNs drives the threshold level of the BNs, so, Eq. (4) now becomes

$$\frac{d^2\theta_i}{dt^2} + \gamma \frac{d\theta_i}{dt} + \omega_o^2(\theta_i - 1) = u(t) = -d\sum_{j=1}^{1} w_{ij} y_i(t) \tag{8}$$

where d is a coefficient that controls the overall coupling strength among the BNs. The coupling weights ω_{ij} are determined by the Hebbian rule as in the case of the PCSMN-2:

$$\omega_{ij} = \sum_{k=1}^{K} \xi_i^k \xi_j^k \tag{9}$$

where $P_k = \{\xi_i^k\}$, $k = 1,2,\ldots,K$ are the K training patterns to be remembered by the network. There are three global parameters to be determined: the amplitude of the relaxation level oscillation ρ_o, the Q-factor of the threshold level dynamics, and the coupling coefficient d. See (25) for detailed discussions on the determination of these parameters.

We carried out a series of simulations of a BNN-1 consisting of 64 BNs. In all the simulations, the same weight matrix encoding 6 random binary patterns was used. For different combinations of network parameters, we repeated 1000 random recall trials in order to investigate the recall characteristics of the network. In each random recall trial, the network was initialized with a random initial state and was allowed to converge to a stable pattern. We counted the number of correct recalls (recall of a stored pattern) and the number of incorrect recalls (recall of a spurious pattern). When the network was not converging to a stable pattern for some time, the network was reinitialized and given another chance to converge to a stable pattern. The results are shown in Table 1. For almost all the combination of the parameters, our network outperformed the Hopfield network (continuous-time). In particular, when ρ_o=0.368, Q=2 and d=0.012, the network successfully recalled a stored pattern without a single exception.

Figure 7 shows the time evolution of the network in one of the correct recall cases. The top plot shows the binary states of all the BNs in the network. The

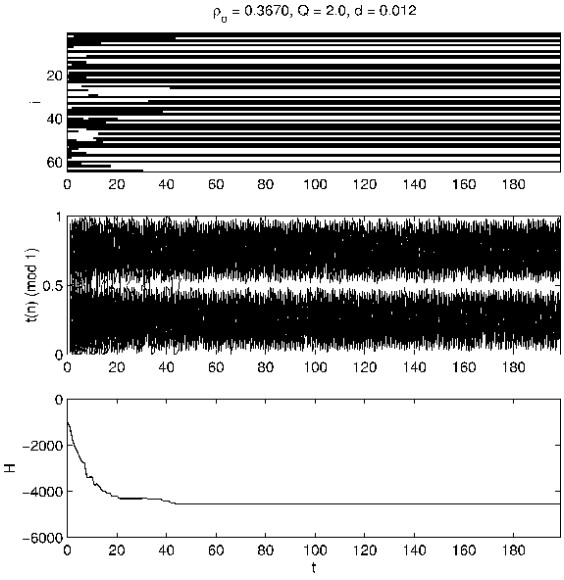

Figure 7 The time evolution of the BNN-1, in one of the correct recall trials: (top) the transition pattern of the binary state variables $s_i(n)$ shown in a black-and-white raster plot, where black represents -1, and white represents 1; (middle) the trajectories of all the firing time series $t_i(n)$; (bottom) the trend of the pseudo-energy function $H(n)$.

Table 1. The recall statistics of the BNN-1: the numbers in the table represent the number of correct recalls of the patterns specified in the column headings.

ρ_o	Q	d	P_1	$\bar{P}_1$	P_2	$\bar{P}_2$	P_3	$\bar{P}_3$	P_4	$\bar{P}_4$	P_5	$\bar{P}_5$	P_6	$\bar{P}_6$	Total
0.367	2.0	0.010	57	90	160	85	117	136	71	69	14	19	68	59	945
0.367	2.0	0.012	52	69	121	85	103	117	138	150	20	22	72	39	988
0.367	20.	0.014	42	74	124	78	105	110	152	157	28	20	57	45	992
0.367	2.5	0.010	38	68	95	51	87	105	163	173	23	30	46	32	911
0.367	2.5	0.012	40	64	104	69	82	94	156	182	30	20	42	29	912
0.367	2.5	0.014	48	67	116	64	93	104	121	139	23	19	46	43	883
0.367	3.0	0.010	34	62	102	42	87	87	124	126	28	24	41	30	787
0.367	3.0	0.012	46	64	104	48	82	91	77	86	28	19	40	31	716
0.367	3.0	0.014	39	64	106	56	93	94	23	17	26	20	38	35	611
0.368	2.0	0.010	58	102	183	116	138	159	47	35	12	8	83	50	991
0.368	2.0	0.012	55	87	152	79	110	130	114	107	21	17	73	55	1000
0.368	2.0	0.014	46	78	143	82	108	127	134	142	22	17	53	46	998
0.368	2.5	0.010	38	64	108	66	96	109	172	181	19	19	51	35	958
0.368	2.5	0.012	34	68	109	59	91	101	163	190	28	19	45	34	941
0.368	2.5	0.014	53	74	124	69	98	107	114	135	24	26	49	40	913
0.368	3.0	0.010	36	69	93	46	92	94	142	162	30	13	42	34	853
0.368	3.0	0.012	44	62	104	54	86	96	87	116	27	19	43	33	771
0.368	3.0	0.014	40	71	98	61	92	93	20	22	23	17	41	35	613

negative state is represented in black, while the positive state is represented in white. Around t=20, the BNs start to form two groups, one with BNs firing in the n-period and the other with BNs firing in the p-period. Such clusters, in fact, exactly correspond to the two groups of BNs that we pictured in Fig. 6. The stabilization of the two groups, therefore, indicates the completion of a recall process. Apparently, the network is still exhibiting chaos, though it is not full-blown. The bottom plot shows the trend of the pseudo-energy function which is defined by

$$H(t) = -\sum_{i=1}^{I}\sum_{j=1}^{I} w_{ij} s_i(t) s_j(t) \qquad (10)$$

An important point to note in the trend of the pseudo-energy function is that it is not always decreasing, but is sometimes increasing to get out of a spurious minimum.

It may be worth looking at what is going on inside the network to convince ourselves of its proper operation. Figure 8 shows the internal state of the first 6 BNs in the network during a recall process. The left and right plots show the state of the BNs in the initial phase and in the final phase of the recall process, respectively. Notice the spontaneous development of sinusoidal oscillation in the threshold level as the recall process proceeds. Initially, the threshold level is flat or

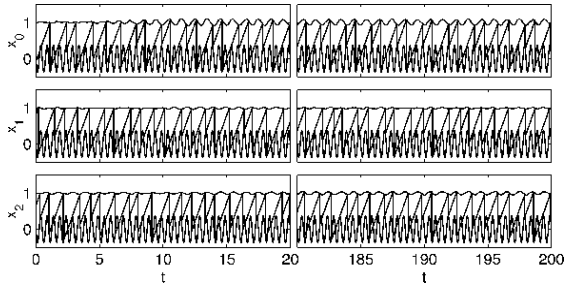

Figure 8 Inside the BNN-1 during recall process: the plots on the left shows the initial, transient behavior of the first 3 BNs while the plots on the right shows the steady-state behavior of the same BNs after a recall process is completed.

random, so the BNs have a chance to switch between the n-period and the p-period freely. As the sinusoidal oscillation develops, the BNs are forced to choose one of the two periods, and in a phase-locked manner.

THE BIFURCATING NEURON NETWORK 2

The BNN-2 is an analog associative memory that can store multiple analog patterns in the time delays of the synapses connecting BNs. In the BNN-2, the firings of all the BNs in the network are phase-locked to the relaxation level oscillation, which is common to all the BNs. Therefore, when the buildup rates of the internal potentials of all the BNs are identical, the firings of all the BNs will be synchronized. An interesting observation is that the firing phase of a BN with respect to the relaxation level oscillation has a proportional relationship with the buildup rate of its internal potential. If an external stimulus representing a spatial pattern affects the buildup rates of the internal potentials of the BNs, the input pattern will be reproduced in the spatial firing-phase pattern of the BNs. In short, the BNs are performing amplitude-to-phase transformation. The amplitude-to-phase transformation function of the BN suggested the possibility of building an analog associative memory out of a BN network. After a firing-phase pattern is formed, inter-BN connections, which induce perturbations in the threshold levels of postsynaptic BNs, can be added to maintain the firing-phase pattern. The firing-phase pattern now forms an attractor of the network, one which has a large basin of attraction.

The BNN-2 has a unique feature that has seldom been exhibited in other integrate-and-fire neuron networks: its memory is dependent on the oscillation frequency of the relaxation level of the BNs. For instance, suppose that a set of patterns is remembered by the network when the relaxation level oscillation frequency is 40Hz. These patterns can only be recalled when the relaxation level oscillation is at 40Hz and cannot be recalled when the frequency is changed, e.g., to 50Hz. After the frequency change, the network can accept new patterns, which can only be recalled when the relaxation level oscillation is at 50Hz. An interesting observation is that the two sets of patterns recorded at different frequencies do not interfere with each other. Such characteristics of the BNN-2's memory are reminiscent of volume holography. The BNN-2 can store multiple pages of memory, and each page can be activated by the tuning of the relaxation level frequency.

Amplitude-to-Phase Transformation of the BN

The following set of equations defines the BN:

$$\frac{dx_i}{dt} = c_i,\ \ \rho(t) = \rho_o \sin 2\pi f t,\ \ \theta_i(t) = 1 \tag{11}$$

where x_i is the internal potential of the neuron while i is the index of the neuron. Note that the sign of the relaxation oscillation $\rho(t)$ is different from the case of the BNN-1. This change is only for the ease of representation and does not change the dynamics of the BN. The firing time of an isolated BN, $t_i(n)$, satisfies the following recursion:

$$t_i(n+1) = t_i(n) + \frac{1}{c_i} - \frac{\rho_o}{c_i}\sin 2\pi f t_i(n) \tag{12}$$

Figure 9 shows the bifurcation diagrams of the firing time $t_i(n)(\mathrm{mod}1)$ of a BN as the bifurcation parameter c_i ranges from 0.5 to 1.5. In the period-1 window of the bifurcation diagrams, which are centered around the point $c_i = 1$, the curve formed by fixed points are given by the following equation:

$$t_i^* = \lim_{n\to\infty} t_i(n) = \frac{1}{2\pi f}\arcsin\frac{1}{\rho_o}\left(1 - \frac{c_i}{f}\right) \tag{13}$$

If we let $c_i = f + u_i$, this becomes

$$t_i^* = \lim_{n\to\infty} t_i(n) = \frac{1}{2\pi f}\arcsin\frac{u_i}{f\rho_o} \tag{14}$$

When $u_i = 0$, t_i^* becomes 0. This means that the BN fires exactly at the beginning of the sinusoidal cycle of

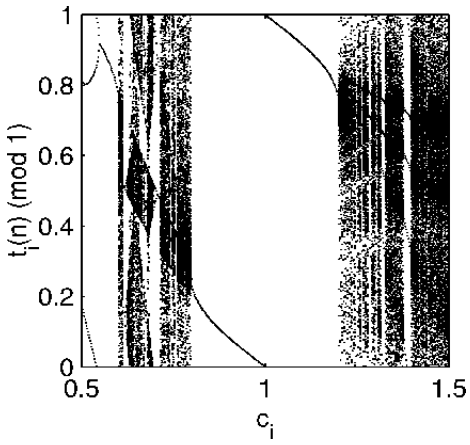

Figure 9 The bifurcation diagrams of the BN with c_i as the bifurcation parameter: the firing time of the BN is approximately in a linear relation with the bifurcation parameter c_i in the period-1 window centered around $c_{i=l}$:f = 1 and $\rho_o = 2$

the relaxation level. As u_i increases, however, a "phase-lead" develops: the spiking of the BN starts to lead the beginning of the sinusoidal cycle. On the other hand, if u_i decreases, a "phase-lag" develops: the spiking of the BN starts to lag behind the beginning of the sinusoidal cycle. In short, the BN is converting an amplitude input to a phase shift in its output spike. Figure 10 illustrates what the amplitude-to-phase transformation implies when it comes to a network of BNs. Since all the BNs in the network are

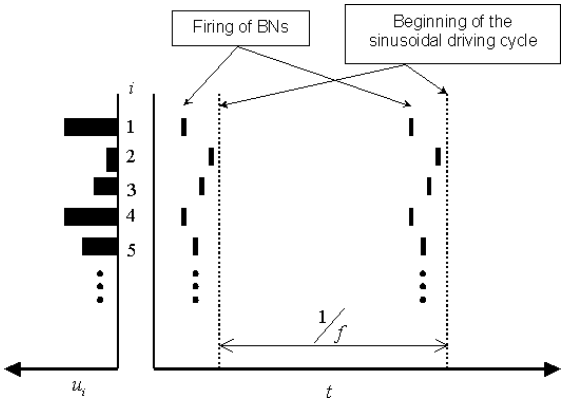

Figure 10 Amplitude-to-phase transformation by BNs: the bars on the left represent inputs to the BNs, and the short, thick lines on the right show the firing times of the BNs.

phase-locked to the sinusoidal oscillation of the relaxation level and will respond to the analog input with a proportional shift in the firing time, we can expect the reproduction of the input pattern in the firing pattern of the BNs as shown in the raster plot on the right side. This figure reminded us of a similar figure that appears in Hopfield (26). He also suggested that a spiking neuron can convert an analog input to a phase shift when it is influenced by an oscillatory drive. It is interesting to see that we arrived at seemingly the same result as his, despite the apparent difference between his neuron model and the BN, our neuron model. However, the detailed conversion characteristics of the BN is difference from that of his model neuron. For instance, the BN performs an almost linear conversion while his model performs a nonlinear conversion, e.g., a logarithmic conversion under a certain condition. Therefore, we would not be able to use the BN to explain the logarithmic intensity transformation of the visual system. Note, however, that linear conversion is better than any other type of conversion, as far as an associative memory is concerned, since it can transfer information with the minimal loss in the presence of noise.

Pulse-Coupling for BNN-2

To begin with, we need to define a coupling mechanism to link BNs. As shown in the previous section, the BN has the capability of amplitude-to-phase transformation of a perturbation u_i in the buildup rate c_i to the firing time of its output spike. Therefore, we will use u_i as an input port: in other words, we will use u_i to denote an external input. The application of an input will induce a firing time pattern in the network, but the pattern will fade away as soon as the input is removed; the network needs interconnections between BNs to maintain an induced firing-time pattern. To this end, we decided to use a threshold coupling :

$$\theta_i(t) = 1 - \delta_i(t) \tag{15}$$

where $\delta_i(t)$ denotes a perturbation in the threshold level induced by inputs from presynaptic BNs. Since the purpose of the threshold coupling is to maintain an induced firing-time pattern, the coupling should have a short time constant so that it is capable of fine time resolution. A simple but effective type of coupling we chose is given by the following first order equation:

$$\frac{d\theta_i}{dt} + \beta(\theta_i - 1) = -du_i^f(t) \tag{16}$$

where β determines the time constant of the restoring dynamics of the threshold level, $u_i^f(t)$ represents the network input, i.e., the input from the presynaptic BNs, and $u_i^f(t)$ is a constant that controls the overall coupling strength of the BNs. The input is the weighted sum of the delayed spike trains from the presynaptic BNs:

$$u_i^f(t) = \sum_{j=1}^{I}\sum_{k=1}^{K} w_{ij}^k y_j(t - \tau_{ij}^k) \tag{17}$$

where the variable $y_i(t)$ represents the output of BN and can be approximated by a series of Dirac-delta functions, each of which represents a spike in the spike train:

$$y_i(t) = \sum_{n=1}^{N_i} \delta(t - t_i(n)) \tag{18}$$

where $t_i(n)$ is the n-th firing time of BN i, and N_i is the ordinal number of the latest firing of BN i. A synaptic connection from BN j to BN i is characterized by the two quantities, w_{ij}^k and τ_{ij}^k: the first represents the strength of the connection, and the second represents the associated time delay. In the current network design, the weight matrix w_{ij}^k is either 1 or 0, only indicating the existence of connection, while the delay matrix τ_{ij}^k can take any real number centered around the average firing period of the BNs for the reason that will soon become clear. The superscript signifies the possibility of repeated connections between a pair of BNs, and it, as it will turn out, is the number of analog patterns to be remembered by the network.

The relaxation level of the BN is subject to a sinusoidal oscillation $\rho(t)$. This relaxation levels of all the BNs in the network are the same. Hereafter, we will call $\rho(t)$ a "driving signal" and, accordingly, ρ_o and f will be called a "driving amplitude" and a "driving frequency", respectively.

A Thought Experiment

Figure 11 illustrates the thought experiment which led us to a possible mechanism to realize an analog associative memory in the BNN-2. The thought experiment is using a simple example network of two BNs. A step-by-step explanation of the experiment follows:

- Initially, no inputs are provided to the BNs. According to Eq. (14), both BNs will be firing exactly at the beginning of the sinusoidal cycle of the driving signal
- A positive external input is provided to BN 2. According to Eq. (14), the spiking of BN 2 will lead that of BN 1 by a small amount. This phase-lead will persist as long as the input is maintained.
- Two time-delayed connections are added: one from BN 1 to BN 2 and the other from BN 2 to BN 1. The lengths of the time delays are determined such that the situation may look as if the firings of both BNs are triggered by each other.
- The input to BN 2 is removed. What will happen now? We expect that the phase-lead of BN2 which was induced by the input will now be maintained by the time-delayed connections.

This experiment suggests a way to embed a memory of a pattern in the BN network. Suppose that the network already contains many connections with a spread of time delays, but of negligibly small strengths. Apply a training pattern to the network. It will develop a phase-lead pattern in the firings of the BNs. While the phase-lead pattern is maintained, we let each BN strengthen those incoming connections

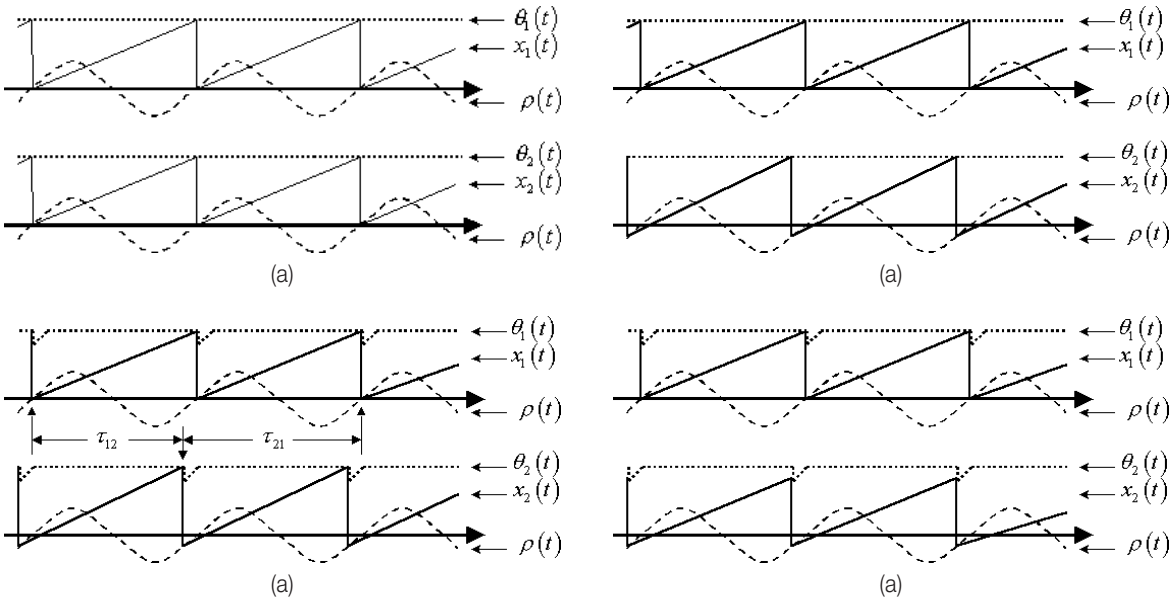

Figure 11 A thought experiment: a network of two BNs illustrates a possible mechanism to realize an analog associative memory using the amplitude-phase transformation characteristics of the BN.

that deliver a spike from other BNs at the exact moment it fires. The phrase, "strengthen those incoming connections that deliver a spike from other BNs at the exact moment it fires." is stating exactly the principle of an online Hebbian training (27).

Analog Associative Memory

Consider a BN network where BNs are arranged in an $L \times L$ planar configuration ($I = L^2$). Each BN is connected to its neighbors that are within the Hemming distance r_c (inclusive). Suppose that the pixel values of a training pattern ξ_i^k are scaled properly and are applied to the network, i.e., $u_i = \gamma f \rho_o \xi_i^k$, where $\gamma<1$ is a positive scaling factor, and f and ρ_o are the frequency and amplitude of the sinusoidal driving signal. The firing times of the BNs are given by Eq. (14), which, when the input u_i is given as above, becomes

$$t_i^* = -\frac{1}{2\pi f}\arcsin\frac{u_i}{f\rho_o} = -\frac{1}{2\pi f}\arcsin\gamma\xi_i^k \qquad (19)$$

Therefore, from the thought experiment in the previous section, the required time delay of the connection from BN j to BN i for the network to maintain the induced phase-lead pattern is given by

$$\tau_{ij}^k = t_i^* - t_j^* + \frac{1}{f} = \frac{1}{f} - \frac{1}{2\pi f}(\arcsin\gamma\xi_i^k - \arcsin\gamma\xi_j^k) \qquad (20)$$

where $1/f$ is added to $t_i^*-t_j^*$ to keep the time delay τ_{ij}^k positive.

Preliminary numerical experiments showed that the behavior of the network is critically dependent on the values of the following parameters: f, t ρ_o, γ, and β. As a matter of fact, the driving frequency f can be chosen to be 1, without loss of generality, by a proper normalization of the time variable. On the other hand, the other parameters should be carefully determined for the optimal performance of the network. See (28) for detailed discussion on the way to determine these parameters.

In order to investigate the recall characteristics of the BNN-2, we carried out a series of computer simulations. In the simulations that follow, we assumed a network of 64 BNs ($I = 64$) arranged in 8×8 planar configuration ($L = 8$).

Simulation 1: multiple attractors in the BNN-2

The purpose of the first simulation is to test if the BN network can remember multiple patterns simultaneously, i.e., the first four patterns in Fig. 12. All the required connections for these patterns are added to the network before the simulation starts. The radius of connection r_c is chosen to be 3, which gives $M = 48$. The other network parameters are chosen as follows: $f = 1$, $\rho_o = 0.1$, $\gamma = 0.5$, $\beta = 200$, and $d = 0.0013$. Simulation results are shown in Fig. 13.

• At $t = 0$, the network is initialized with a random state, i.e., the internal potential of the BNs are initialized with random numbers.

• At $t = 50$, the first training pattern ξ_i^l is applied to the network. At $t = 75$, the input is removed.

• The above two steps are repeated for the remaining training patterns.

• At $t = 250$, a random pattern, which is not one of the four training patterns, is applied to the network as an input.

• At $t = 275$, the input is removed.

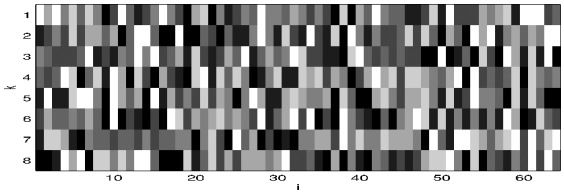

Figure 12 Training patterns used in the simulations of the BNN-2: pixel values are represented in grayscale: black represents 0, and white represents 1.

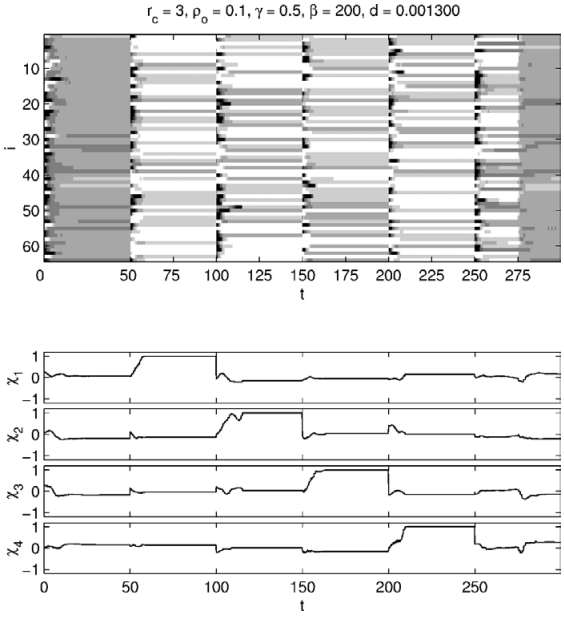

Figure 13 Simulation 1: (top) the time evolution pattern of the BNN-2 shown in a gray-scale raster plot, where black represents a firing-time lead of 0.05, and white represents a firing-time lag of 0.05, and (bottom) the change of the correlation $x_k(t)$ in time.

Figure 13 contains two types of plots: a raster plot and a line plot. The raster plot shows the lead in the firing time of each BN which is defined by

$$\zeta_i(t) = -\rho(t_i(t)) = -\rho_o \sin 2\pi f t_i(t) \tag{21}$$

where $t_i(t)$ is the time of the last firing of BN i before t. The line plot shows the correlation between the phase-lead pattern of the network and one of the four training patterns during the simulation:

$$x_k(t) = \frac{\sum_{i=0}^{I}(\xi_i^k - \bar{\xi}^k)(\zeta_k(t) - \bar{\zeta}(t))}{\sqrt{\sum_{i=0}^{I}(\xi_i^k - \bar{\xi}^k)^2 \sum_{i=0}^{I}(\zeta_k(t) - \bar{\zeta}(t))^2}} \tag{22}$$

where $\bar{\xi}^k = \frac{1}{I}\sum_{i=1}^{I}\xi_i^k$ and $\bar{\zeta}(t) = \frac{1}{I}\sum_{i=1}^{I}\zeta(t)$. We can observe a marked difference in the responses of the network to a known pattern and an unknown pattern. A phase-lead pattern induced by a known pattern persists after the removal of the input until a new input is applied. The response of the network is completely different for an unknown pattern: the network forgets the pattern as soon as the input is removed.

Simulation 2: large basins of attraction?

Simulation 1 demonstrated the basic memory capability of the BNN-2. However, this alone is not sufficient to make the BNN-2 a useful associative memory since an associative memory should be able to recognize a pattern which is known but is distorted by noise. Also, the entire input pattern sometimes may not be available, and an associative memory is required to complete the entire pattern from a part of

it. In terms of nonlinear dynamics, this problem reduced to that of the size of a basin of attraction: we need to examine how large are the basins of attraction associated with the attractors. The choice of the network parameter values used in this simulation is as follows: $r_c = 3$, $f = 1$, $\rho_o = 0.1$, $\gamma = 0.5$, $\beta = 300$, and $d = 0.0025$.

We prepared corrupted versions of the first four training patterns, which was shown in Fig. 12, for this simulation.

$$\tilde{\xi}_i^k = \begin{cases} \xi_i^k & i \le I/2 \\ 0 & i > I/2 \end{cases} \quad \text{h} \tag{23}$$

The first half of each corrupted version is the same as that of the corresponding original pattern, and the second half is filled with zeros. All the connections with the required time delays for the four original training patterns are established in advance.

• At $t = 0$, the corrupted version of the first training pattern is applied to the network as an input. Then, the network is allowed to run until $t = 50$ so that it can reconstruct the whole pattern.

• The above step is repeated for the other corrupted training patterns: the second at $t = 50$, the third at $t = 100$, and the fourth at $t = 150$.

Simulation results are shown in Fig. 14. We can see an apparent visual difference in the pattern of the network response to the inputs in the first and the second half of the network. A longer transient period in the second half of the network indicates the network's effort to reconstruct the missing part in the input patterns. When $\beta = 200$, the network could reconstruct the missing part successfully for the first, third and fourth training patterns but not for the second pattern. To obtain a better performance of the network, we had to test with many other combinations of the network parameters, and the result shown in Fig. 14 is one of the outcomes: the network is now successful for all of the training patterns. It seemed that the network tends to perform better when the parameter β is larger. However, the network model will depart further from biological reality if the parameter β becomes too large.

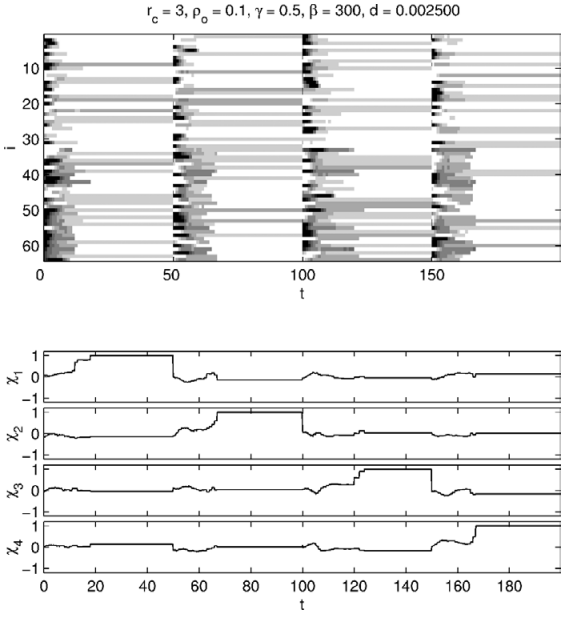

Figure 14 Simulation 2: (top) the time evolution pattern of the BNN-2 shown in a gray-scale raster plot, where black represents a firing-time lead of 0.05, and white represents a firing-time lag of 0.05, and (bottom) the change of the correlation $x_k(t)$ in time.

Simulation 3: volume-holographic memory 1

According to Eq. (20), the time delays associated with the connections required to store a pattern in the BNN-2 are dependent on the driving frequency f. This means that the network's recall of a stored pattern is only possible when the same driving signal that was present at the time of training is present. This situation is reminiscent of volume holography (29). For a volume hologram to reconstruct a recorded image, it is necessary that a reference beam should be supplied exactly at the same angle as it was in the recording step. In fact, this sensitivity to the angle of the reference beam enables volume holography to store multiple patterns in a single refractive crystal. It appears that the driving frequency f of the BNN-2 plays the role of the angle of a reference beam in volume holography. Therefore, the question which we

are about to answer in the simulation is this: can the BNN-2 store different patterns at different driving frequencies without causing interference among the patterns? The values of the network parameters used in this simulation are as follows: $r_c = 3$, $f = 1$, $\rho_o = 0.1$, $\gamma = 0.5$, $\beta = 300$, and $d = 0.003$.

The results are shown in Fig. 15. The time-delayed connections for the first four training patterns shown in Fig. 12 are added to the network in advance. In doing so, we used different driving frequencies for different training patterns: $f = 1$, 1.02, 1.04 and 1.06 for the four training patterns, respectively. At $t = 0$, the network is randomized, i.e., the internal potentials of the BNs are initialized with random numbers. While the simulation is running, the frequency of the driving signal is changed discontinuously in the following order: $f = 1$ at $t = 0$, $f = 1.02$ at $t = 50$, $f = 1.04$ at $t = 100$, and $f = 1.06$ at $t = 150$. Each of the four embedded patterns shows up when the driving frequency is switched to the frequency which was assumed when the pattern was added to the network.

Simulation 4: volume-holographic memory 2

This simulation is a slight variation of simulation 3. In this simulation, we used all of the eight training patterns shown in Fig. 12: the first four and the second four training patterns added to the network assuming driving frequencies of $f = 1$ and 1.02, respectively. We designed this simulation in order to check if the two memory spaces associated with the two different driving frequencies are independent and do not interfere. Simulation results are shown in Fig. 16.

- At $t = 0$, the network is initialized with a random state, i.e., the internal potential of the BNs are initialized with random numbers.
- At $t = 50$, the first training pattern is applied to the network.
- At $t = 75$, the input is removed.
- The above two steps are repeated for the remaining training patterns.

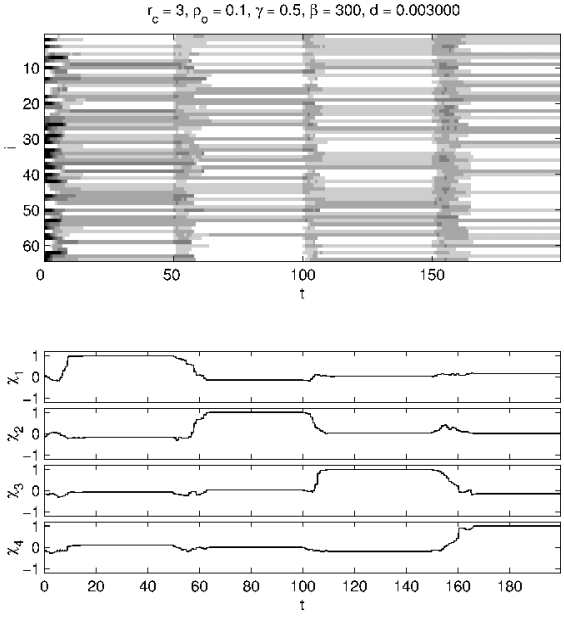

Figure 15 Simulation 3: (top) the time evolution pattern of the BNN-2 shown in a gray-scale raster plot, where black represents a firing-time lead of 0.05, and white represents a firing-time lag of 0.05, and (bottom) the change of the correlation $x_k(t)$ in time.

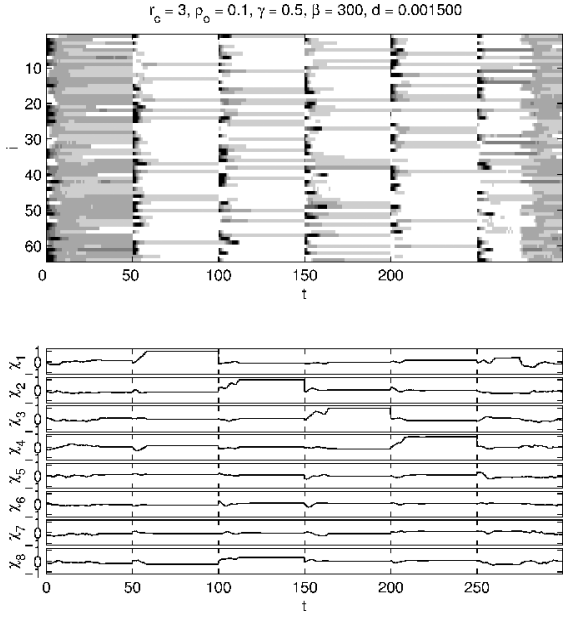

Figure 16 Simulation 4: (top) the time evolution pattern of the BNN-2 shown in a gray-scale raster plot, where black represents a firing-time lead of 0.05, and white represents a firing-time lag of 0.05, and (bottom) the change of the correlation $x_k(t)$ in time.

- At $t = 250$, the fifth pattern, which is one of the four training patterns which were embedded in the network assuming the driving frequency of 1.02, is applied to the network.
- At $t = 275$, the input is removed.

Throughout the simulation, the driving frequency was kept constant at $f = 1$. Up to our expectation, the network can not recognize the fifth pattern which was added to the network assuming a different driving frequency ($f = 1.02$). The network is treating the fifth pattern in the same way as it did a random pattern in simulation 1. This experimental result clearly demonstrates the independence of the memory spaces associated with different driving frequencies.

DISCUSSIONS

In the beginning, we pointed out that the three new issues in neuroscience, namely, time coding, the role of coherent activity, and the role of chaotic activity, motivated the design of the BN networks. Now, based on what we have observed in the BN networks, we are tempted to talk back to biology despite the risk of being purely hypothetical.

- The BNs in the networks can communicate with each other, i.e., decode the information conveyed by spike trains only because they have a common time reference. This observation suggests that a coherent activity may be a necessary condition, in a network where time coding is used, for an intensive information transaction among neurons.
- The BNN-1 suggests a possible role of chaos. Chaos in the BNN-1 is a natural source of noise that goes away after perception, and also allows a network to have more symbols for expression. Also, attractor merging crisis enables transition between searching and perception more rapid than an exponential convergence.
- In the BNN-2 the frequency of the sinusoidal oscillation can be adjusted to put the network into different independent modes. If we consider a large network consisting of a number of functionally independent sub-networks, we will be able to selectively activate a certain function of the network by "illuminating" the corresponding sub-network with a sinusoidal signal. This scenario is in fact reminiscent of the searchlight hypothesis of Crick (13).
- In the BNN-1 and 2, the average firing rate of every BN is always 1, before or after the convergence of the network. If a real biological neural network is operating in a fashion similar to that of the BNNs, the measurement of the average firing rate of neurons in the network will reveal no sign of meaningful activity although the network is indeed involved in an active computing task.
- The BNN-1 is always operating in a chaotic state, which means that the inter-spike intervals of the individual BNs can never be constant. Softky and Kock (30) reported high variability of the inter-spike intervals in their analysis of data from the cat and the primary visual cortex (V1) and extra-striate cortex (MT) neurons. Their finding was inconsistent with the neural networks that are based on the original integrate-and-fire neuron model (22), but are, apparently, in agreement with the BNN-1.

REFERENCES

1. Adrian ED. The impulses produced by sensory nerve endings. Journal of Physiology 1926; 61: 49-72.
2. Rieke F, Warland D, Ruyter van Steveninck Rd, Bialek W. Spikes - Exploring the Neural Code, Cambridge, MA: MIT Press, 1996.
3. O' Keefe J, Recce ML. Phase relationship between hippocampal place units and the EEG theta rhythm. Hippo campus 1993; 3: 317-330.
4. O' Keefe J, Dostrovsky J. The hippocampus as a spatial map: preliminary evidence from unit activity in the freely-moving rat. Brain Research 1971; 34: 171-175.

5. Freeman W, Skarda CA. Spatial EEG patterns, nonlinear dynamics and perception: neo-Sherringtonian view. Brain Research Reviews 1985; 10: 147-175.
6. Bressler SL, Freeman WJ. Frequency analysis of olfactory system EEG in cat, rabbit, and rat. Electroencephalography and Clinical Neurophysiology 1980; 50: 19-24.
7. Gray CM, Singer W. Stimulus-specific neuronal oscillations in orientation columns of cat visual cortex. Proceedings of the National Academy of Sciences of the USA 1989; 86: 1698-1702.
8. Eckhorn R, Bauer R, Jordan W, Brosch M, Kruse W, Munk M, Reitboeck HJ. Coherent oscillations: a mechanism of feature linking in the visual cortex? Biological Cybernetics 1988; 60: 121-130.
9. Freeman W, van Dijk BW. Spatial patterns of visual cortical fast EEG during conditioned reflex in a rhesus monkey. Brain Research 1987; 422: 267-276.
10. Krieger D, Dillbeck M. High frequency scalp potentials evoked by a reaction time task. Electroencephalography and Clinical Neurophysiology 1987; 67: 222-230.
11. Milner PM. A model for visual shape recognition. Psychology Review 1974; 81: 521-535.
12. von der Malsburg C. The correlation theory of brain function. In: Domany E, van Hemmen JL et al. , eds. Models of Neural Networks II. Springer-Verlag, 1994: .
13. Crick F. Function of the thalamic reticular complex: the searchlight hypothesis. Proceedings of the National Academy of Sciences of the USA 1984; 81: 4586-4590.
14. Rapp PE, Zimmerman ID, Albano AM, Deguzman GC, Greenbaum NN. Dynamics of spontaneous neural activity in the simian motor cortex: the dimension of chaotic neurons. Physics Letters A 1985; 110: 335-338.
15. Babloyantz A, Nicolis C, Salazar M. Evidence of chaotic dynamics of brain activity during the sleep cycle. Physics Letters A 1985; 111: 152-156.
16. Babloyantz A, Destexhe A. Low-dimensional chaos in an instance of epilepsy. Proceedings of the National Academy of Sciences of the USA 1986; 83: 3513-3517.
17. Freeman W. Petit mal seizure spikes in olfactory bulb and cortex caused by runaway inhibition after exhaustion of excitation. Brain Research Reviews 1986; 11: , 259.
18. Skarda CA, Freeman WJ. How Brains Make Chaos in Order to Make Sense of the World. Behavioral Brain Research 1987; 10: 161-195.
19. Yao Y, Freeman WJ. Model of biological pattern recognition with spatially chaotic dynamics. Neural Networks 1990; 3: 153-170.
20. Nicolis J. Chaotic dynamics applied to information processing. Reports on Progress in Physics 1986; 49: 1109-1196.
21. Nicolis JS. Chaos and Information Processing: A Heuristic Outline, Singapore, Teaneck, NJ: World Scientific, 1991.
22. Knight BW. Dynamics of encoding in a population of neurons. Journal of General Physiology 1972; 59: 734-766.
23. Rabinovich MI, I. Abarbanel HD. The role of chaos in neural systems. Neuroscience 1998; 87: 5-14.
24. Grebogi C, Ott E, Romeiras F, Jorke JA. Critical exponents for crisis-induced intermittency. Physical Review A 1987; 36: 5365-5380.
25. Lee G, Farhat NH. The bifurcating neuron network 1. Neural Networks 2001; 14: 109-125.
26. Hopfield JJ. Pattern recognition computation using action potential timing for stimulus representation. Nature 1995; 376: 33-36.
27. Hebb DO. The organization of behavior: a neuropsychological theory, New York: Wiley, 1949.
28. Lee G, Farhat NH. The Bifurcating Neuron Network 2: an analog associative memory. Neural Networks 2002; 15: 55-70.
29. Psaltis D, Brady D, X-G. Gu, Lin S. Holography in artificial neural networks. Nature 1990; 343: .
30. Softky WR, Koch C. The highly irregular firing of cortical cells is inconsistent with temporal integration of random EPSPs. Journal of Neuroscience 1993; 13: 334-350.